

Designing metachronal waves of cilia

Fanlong Meng,^{1,2,*} Rachel R. Bennett,^{3,4,*} Nariya Uchida,⁵ and Ramin Golestanian^{2,4,†}

¹*CAS Key Laboratory for Theoretical Physics, Institute of Theoretical Physics,
Chinese Academy of Sciences, Beijing 100190, China*

²*Max Planck Institute for Dynamics and Self-Organization (MPIDS), Göttingen 37077, Germany*

³*School of Mathematics, University of Bristol, Bristol BS8 1TW, UK*

⁴*Rudolf Peierls Centre for Theoretical Physics, University of Oxford, Oxford OX1 3NP, UK*

⁵*Department of Physics, Tohoku University, Sendai, 980-8578, Japan*

(Dated: March 12, 2021)

On surfaces with many motile cilia, beats of the individual cilia coordinate to form metachronal waves. We present a theoretical framework that connects the dynamics of an individual cilium to the collective dynamics of a ciliary carpet via systematic coarse-graining. We uncover the criteria that control the selection of frequency and wavevector of stable metachronal waves of the cilia and examine how they depend on the geometric and dynamical characteristics of single cilia, as well as the geometric properties of the array. We perform agent-based numerical simulations of arrays of cilia with hydrodynamic interactions and find quantitative agreement with the predictions of the analytical framework. Our work sheds light on the question of how the collective properties of beating cilia can be determined using information about the individual units, and as such exemplifies a bottom-up study of a rich active matter system.

Motile cilia are hair-like organelles that beat with a whip-like stroke that breaks time-reversal symmetry to create fluid flow or propel swimming microorganisms under low Reynolds number conditions [1–3]. The beat is actuated by many dynein motors, which generate forces between microtubules that cause the cilium to bend in a robust cyclic manner with moderate fluctuations [4, 5]. On surfaces with many cilia, the actuating organelles can coordinate with each other and collectively beat in the form of a metachronal waves, where neighboring cilia beat sequentially (i.e. with a phase lag) rather than synchronously [6]. The flows created from this coordinated beating are important for breaking symmetry in embryonic development [7, 8], creation of complex and dynamic flow patterns for the cerebrospinal fluid in the brain [9, 10], and providing access to nutrients [11]. In microorganisms such as *Paramecium* and *Volvox*, the metachronal beating of cilia provides propulsion strategies in viscous environments [12, 13]. It has been shown that depending on the parameters beating ciliary carpets can exhibit globally ordered and turbulent flow patterns [14], which can be stable even with a moderate amount of quenched disorder [15], and that metachronal coordination optimizes the efficiency of fluid pumping [16, 17]. Natural cilia have inspired various designs of artificial cilia [18–22], which may be used for pumping fluid [23, 24] and mixing [25], or fabrication of microswimmers [26].

Hydrodynamic interactions have been shown to play a key role in coordinated beating of cilia [27, 28] and mediating cell polarity control [29]. To achieve synchronization between two cilia via hydrodynamic interactions, it is necessary to break the permutation symmetry between them, e.g. by exploiting the dependence of the drag co-

efficient on the distance from a surface [30], flexibility of the anchoring of the cilia [31], non-uniform beat patterns [32, 33], or any combination of these effects [34]. In addition to the hydrodynamic interactions, the basal coupling between cilia can also facilitate the coordination [35–37].

How can we predict the collective behavior of arrays of many cilia coordinated by hydrodynamic interactions, and in particular the properties of the emerging metachronal waves, from the single-cilium characteristics? Extensive numerical simulations using explicitly resolved beating filaments [16, 17, 27, 38–40] and simplified spherical rotors [13, 14, 41, 42] have demonstrated that metachronal coordination emerges from hydrodynamic interactions. However, insight into this complex many-body dynamical system at the level that has been achieved in studies of two cilia is still lacking. Here, we propose a theoretical framework for understanding the physical conditions for coordination of many independently beating cilia, which are arranged on a substrate in the form of a 2D array immersed in a 3D fluid. We uncover the physical conditions for the emergence of stable metachronal waves, and predict the properties of the wave in terms of single-cilium geometric and dynamic characteristics.

RESULTS

We use a simplified model of a cilium as a force monopole moving along a circular trajectory of radius a above a substrate, as shown in Fig. 1(a). To theoretically study metachronal coordination, we consider such model cilia on a lattice of spacing ℓ in the x - y plane as shown in Fig. 1(b). We examine the role of the geometric parameters in determining the collective mode of coordination. We parametrize the orientation of the cilia by the angle θ that the plane of the circular trajectory

* F. M. and R. R. B. contributed equally to this work.

† ramin.golestanian@ds.mpg.de

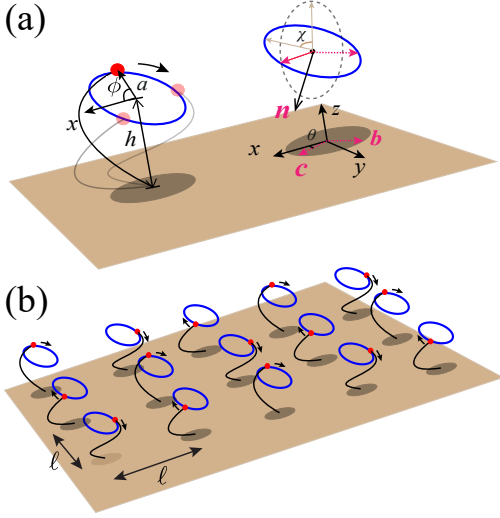


FIG. 1. (a) Simplified description of a single cilium as represented by a force-monopole with a cyclic trajectory above a rigid substrate. Various geometric measures and orientation vectors are defined in the figure. (b) An array of cilia on a square lattice in the x - y plane with the lattice constant ℓ .

makes with the \mathbf{e}_x direction, and the tilt angle χ it makes with the \mathbf{e}_z direction. More concretely, we define the vector $\mathbf{c} = (\cos \theta, \sin \theta, 0)$ to characterize the 2D orientation of the circular orbit and $\mathbf{b} = (-\sin \theta, \cos \theta, 0)$, which is perpendicular to \mathbf{c} , and the unit vector that is normal to circular trajectory is defined as $\mathbf{n} = -\cos \chi \mathbf{b} - \sin \chi \mathbf{e}_z$; see Fig. 1(a). The position of the sphere representing the force monopole along the trajectory, which we parametrize by the polar angle ϕ_i for the i th sphere, is

$$\mathbf{R}_i = \mathbf{r}_i + h\mathbf{e}_z + a \cos \phi_i \mathbf{c} + a \sin \phi_i (-\sin \chi \mathbf{b} + \cos \chi \mathbf{e}_z), \quad (1)$$

where $\mathbf{r}_i = (x_i, y_i, 0)$ denotes the lattice coordinate (with spacing ℓ) and h denotes the distance from the center of the trajectory to the substrate. There are also simulation studies adopting non-circular trajectories of the cilia, and interested readers can refer to Ref. [13, 30, 42, 43].

Dynamical equations

Each cilium is driven independently by a tangential force acting on the bead. The magnitude of the force, $f(\phi_i)$, depends only on the location of the bead along its trajectory, and the direction of the force is given by the tangent vector, which is defined as

$$\mathbf{t}_i(\phi_i) = \frac{d\mathbf{R}_i/d\phi_i}{|d\mathbf{R}_i/d\phi_i|}. \quad (2)$$

The friction coefficient of the bead, $\zeta(\phi_i)$, can, in general, depend on the location of the bead along the trajectory, e.g. due to the proximity of a substrate. Balancing the forces for a single cilium, we find that the velocity of

the bead is $\mathbf{v}_i = \dot{\phi}_i a \mathbf{t}_i = f(\phi_i)/\zeta(\phi_i) \mathbf{t}_i$. In an array, the hydrodynamic interactions between the cilia will also influence the beating, leading to a system of coupled dynamical governing equations for the phase variables

$$\frac{d\phi_i}{dt} = \frac{f(\phi_i)}{\zeta(\phi_i)a} + \frac{1}{a} \sum_j \mathbf{t}_i(\phi_i) \cdot \mathbf{G}(\mathbf{R}_i, \mathbf{R}_j) \cdot \mathbf{t}_j(\phi_j) f(\phi_j) \mathbf{3} \quad (3)$$

where the the Green's function $\mathbf{G}(\mathbf{R}, \mathbf{R}')$ (the Blake tensor) represents the hydrodynamic effect in an incompressible fluid of a force-monopole located at \mathbf{R}' at the observation point \mathbf{R} in the presence of a substrate with no-slip boundary condition [44].

The intrinsic angular speed of each cilium given as

$$\Omega(\phi) = f(\phi)/[\zeta(\phi)a], \quad (4)$$

can generically have phase dependence arising from the stroke pattern of the beating, which can be represented via its harmonics as

$$f(\phi) = f_0 [1 + \sum_{n=1} A_n \cos n\phi + B_n \sin n\phi], \quad (5)$$

and the cyclic change in the friction, which we represent as

$$\zeta(\phi) = \zeta_0 [1 + \sum_{n=1} C_n \cos n\phi + D_n \sin n\phi]. \quad (6)$$

The scale of the friction coefficient can be written as $\zeta_0 = 4\pi\eta b$, where the length scale b represents the characteristic (hydrodynamic) size of a cilium. Naturally, the harmonic amplitudes are constrained to values that will correspond to strictly positive values for the force and the friction coefficient. To proceed with the analysis of (3), we introduce a coordinate transformation $\phi \rightarrow \bar{\phi}$, defined via the following relation:

$$\frac{d\bar{\phi}}{d\phi} = \frac{\Omega(\phi)}{\Omega_0}, \quad (7)$$

where $\Omega_0 = f_0/(\zeta_0 a)$ is a constant angular speed describing the free dynamics of the new coordinate [32]. The definition can be integrated to obtain the relation between the coordinates as

$$\phi(\bar{\phi}) \simeq \bar{\phi} + \sum_{n=1} \frac{1}{n} [(A_n - C_n) \sin n\bar{\phi} - (B_n - D_n) \cos n\bar{\phi}], \quad (8)$$

to the lowest order in the harmonic amplitudes.

Using the translational invariance along the substrate, we can express the Blake tensor in the 2D Fourier space $\mathbf{q} = (q_x, q_y, 0) \equiv q\hat{\mathbf{q}}$ (see Supplemental Material for the details of the derivation) and recast Eq. (3) in terms of the the new coordinate. We then use a separation of time scale between the mean-phase and the phase-difference to simplify the dynamics. By changing the notation from $\phi_i(t)$ to $\phi(\mathbf{r}, t)$ and averaging over the fast variables, the governing dynamical equation can be written as [45]

$$\partial_t \bar{\phi}(\mathbf{r}, t) = \Omega_0 + \frac{\Omega_0 h b}{16\pi} \sum_{\mathbf{r}'} \int d^2 \mathbf{q} e^{i\mathbf{q} \cdot (\mathbf{r} - \mathbf{r}')} \quad (9)$$

$$\times [\mathcal{M}(\mathbf{q}) \cos(\bar{\phi}(\mathbf{r}) - \bar{\phi}(\mathbf{r}')) + \mathcal{S}(\mathbf{q}) \sin(\bar{\phi}(\mathbf{r}) - \bar{\phi}(\mathbf{r}'))],$$

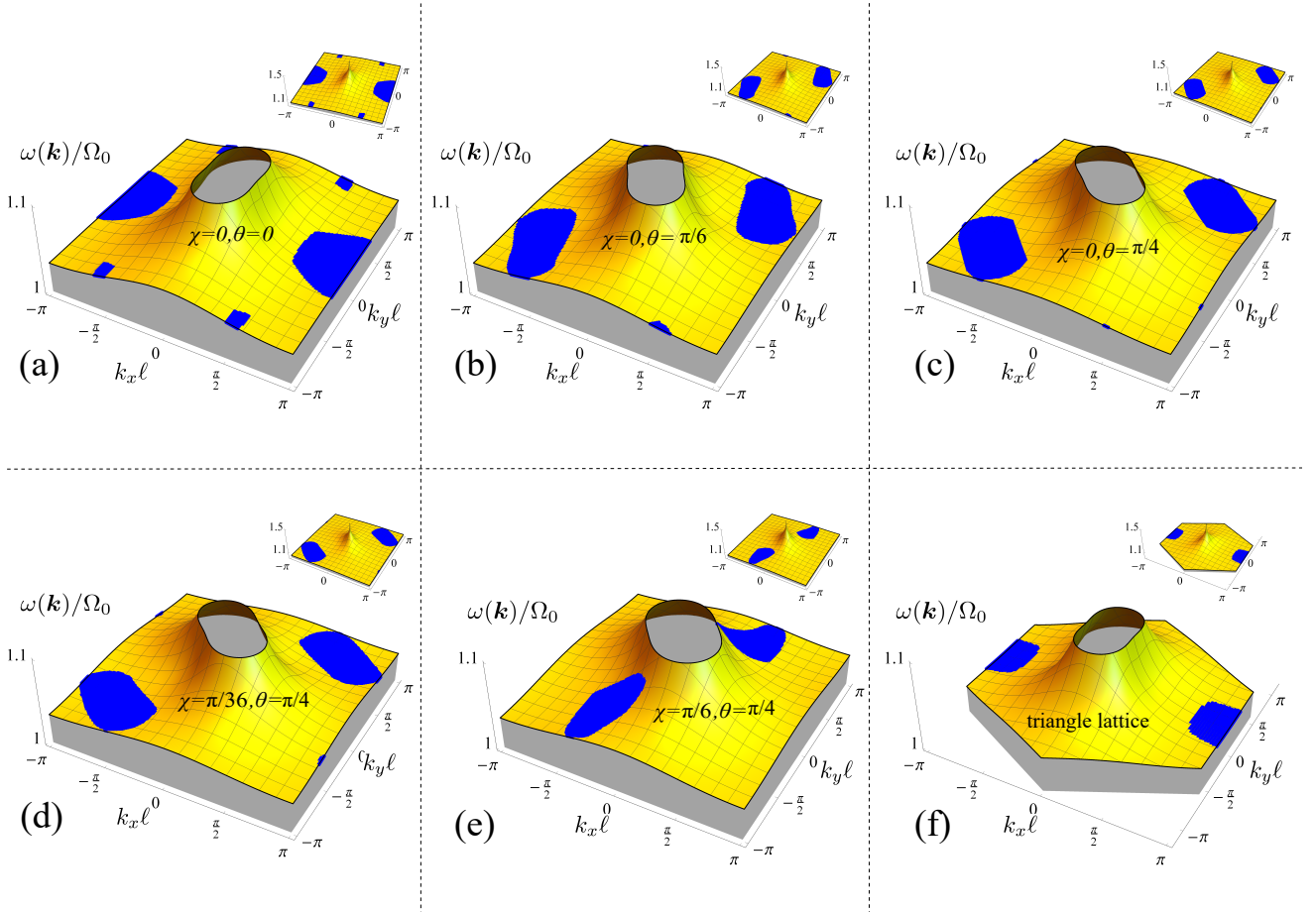


FIG. 2. Dispersion relation of the metachronal waves. The (non-dimensionalized) frequency $\omega(\mathbf{k})/\Omega_0$ defined in Eq. (12) is plotted as a function of the wave vector $(k_x\ell, k_y\ell)$ in the first Brillouin zone. Panels (a)-(e) correspond to a ciliary array on a square lattice with the following trajectory orientation and tilt angles: (a) $\chi = 0, \theta = 0$, (b) $\chi = 0, \theta = \pi/6$, (c) $\chi = 0, \theta = \pi/4$, (d) $\chi = \pi/36, \theta = \pi/4$ and (e) $\chi = \pi/6, \theta = \pi/4$. Panel (f) corresponds to a triangular lattice with $\chi = 0, \theta = 0$. Other parameters for panels (a)-(f) are: $a = 0.2\ell, b = 0.05\ell, h = \ell, A_2 = 0.5, B_2 = 0.5, C_2 = 0$, and $D_2 = 0$. Blue shaded regions denote the stable wave zones as determined by the linear stability analysis from Eq. (13).

where the \mathbf{q} -dependent kernels are defined as

$$\begin{aligned} \mathcal{M} &= g_0(\mathbf{q}h) + g_1(\mathbf{q}h)(A_2 - 2C_2) + g_2(\mathbf{q}h)(B_2 - 2D_2) \\ \mathcal{S} &= g_1(\mathbf{q}h)(2B_2 - D_2) - g_2(\mathbf{q}h)(2A_2 - C_2), \end{aligned} \quad (11)$$

in terms of the following functions:

$$\begin{aligned} g_0(\mathbf{p}) &= 2p^{-1}[e^{-2p(a/h)} - e^{-2p}][3 - \cos^2\chi(\hat{\mathbf{p}} \cdot \mathbf{c})^2] \\ &\quad + 4(1-p)e^{-2p}[1 - \cos^2\chi(\hat{\mathbf{p}} \cdot \mathbf{b})^2] \\ &\quad - 4(1+p)e^{-2p}\cos^2\chi, \\ g_1(\mathbf{p}) &= p^{-1}[e^{-2p(a/h)} - e^{-2p}][(\hat{\mathbf{p}} \cdot \mathbf{b})^2 - \sin^2\chi(\hat{\mathbf{p}} \cdot \mathbf{c})^2] \\ &\quad - 2(1-p)e^{-2p}[(\hat{\mathbf{p}} \cdot \mathbf{c})^2 - \sin^2\chi(\hat{\mathbf{p}} \cdot \mathbf{b})^2] \\ &\quad - 2(1+p)e^{-2p}\cos^2\chi, \\ g_2(\mathbf{p}) &= 2\{p^{-1}[e^{-2p(a/h)} - e^{-2p}] - 2(1-p)e^{-2p}\}\sin\chi(\hat{\mathbf{p}} \cdot \mathbf{b})(\hat{\mathbf{p}} \cdot \mathbf{c}). \end{aligned}$$

Importantly, we find that only the second harmonics in the beat pattern and the friction cycle play a key role in determining the collective behavior of the cilia at long time scales. The compact form of Eq. (9) allows us to sys-

tematically investigate the conditions under which the array of cilia can admit stable metachronal wave solutions, and what determines the direction of propagation and the wavelength of the wave. As we shall see below, $\mathcal{M}(\mathbf{q})$ will determine the characteristics of the metachronal waves and $\mathcal{S}(\mathbf{q})$ will determine their stability.

Dispersion relation

Let us now consider a situation where the cilia beat in coordination and generate a metachronal wave of frequency ω and wavevector \mathbf{k} . We describe the traveling wave as $\bar{\phi}(\mathbf{r}, t) = \omega t - \mathbf{k} \cdot \mathbf{r} + \delta\bar{\phi}_{\mathbf{k}}(\mathbf{r}, t)$, where $\delta\bar{\phi}_{\mathbf{k}}$ represents perturbations around the harmonic traveling wave *ansatz*. Evaluating Eq. (9) at the zeroth order, and making use of the identity $\sum_{\mathbf{r}, \mathbf{r}'} e^{i\mathbf{q} \cdot (\mathbf{r} - \mathbf{r}')} = \sum_{\mathbf{G}} \frac{4\pi^2}{\ell^2} \delta^2(\mathbf{q} + \mathbf{G})$ where \mathbf{G} represents the reciprocal lattice vectors, we find

the dispersion relation of the metachronal waves as

$$\omega(\mathbf{k}) = \Omega_0 \left[1 + \frac{\pi}{4} \frac{hb}{\ell^2} \sum_{\mathbf{G}} \mathcal{M}(\mathbf{k} + \mathbf{G}) \right]. \quad (12)$$

We recall, for example, that for a square lattice we have $\mathbf{G} = \frac{2\pi}{\ell}(m\mathbf{e}_x + n\mathbf{e}_y)$ for $m, n \in \mathbb{Z}$.

The dispersion relation is plotted in Fig. 2 for various choices of cilia orientation. Note that the resulting frequencies for all modes are somewhat larger than the single cilium frequency Ω_0 , due to a renormalization of the frequency by hydrodynamics interactions. For example, $\omega(\mathbf{0})/\Omega_0 = 1 + \frac{\pi}{4} \frac{hb}{\ell^2} \sum_{\mathbf{G}} \mathcal{M}(\mathbf{G}) \approx 1.43$ for the parameter set corresponding to Fig 2(a), namely, $\theta = 0$, $\chi = 0$, $h = \ell$, $a = 0.2\ell$, $b = 0.05\ell$, $A_2 = 0.5$, $B_2 = 0.5$, $C_2 = 0$, and $D_2 = 0$.

Stability criterion

Satisfying the dispersion relation provides a necessary condition for frequencies and wavevectors to represent metachronal waves. However, it does not guarantee that the wave is a stable solution to Eq. (9). To check the stability of a solution, we can expand Eq. (9) in terms of $\delta\bar{\phi}_{\mathbf{k}}$, and probe the first order governing equation for the perturbation. In Fourier space, we find the time evolution of a perturbation with wavevector \mathbf{q} in a background of uniform wave with wavevector \mathbf{k} to satisfy the following equation

$$\partial_t \delta\bar{\phi}_{\mathbf{k}}(\mathbf{q}) = - \left[\Gamma(\mathbf{q}, \mathbf{k}) - \Gamma(\mathbf{0}, \mathbf{k}) \right] \delta\bar{\phi}_{\mathbf{k}}(\mathbf{q}), \quad (13)$$

where

$$\Gamma(\mathbf{q}, \mathbf{k}) = \frac{\pi b \Omega_0}{8\ell^2} \sum_{\mathbf{G}} [\mathcal{S}(\mathbf{q} + \mathbf{k} - \mathbf{G}) + \mathcal{S}(\mathbf{q} - \mathbf{k} - \mathbf{G})]. \quad (14)$$

The sign of $\Gamma(\mathbf{q}, \mathbf{k}) - \Gamma(\mathbf{0}, \mathbf{k})$ determines whether the background wave solution with wavevector \mathbf{k} is stable with respect to a perturbation with wavevector \mathbf{q} . If $\Gamma(\mathbf{q}, \mathbf{k}) - \Gamma(\mathbf{0}, \mathbf{k}) > 0$ for all values of \mathbf{q} , then the background metachronal wave with wavevector \mathbf{k} is linearly stable.

In Fig. 2, the wavevectors corresponding to linearly stable solutions of Eq. (9) are shown as (blue) dots. The explicit expression for \mathcal{S} allows us to make predictions about the necessary criteria for the stability of the waves. For example, when $\chi = 0$ stability requires the condition $2B_2 - D_2 > 0$ to be satisfied. In this case, one can generally observe that the stable modes propagate along the direction of the ciliary beating with wavelengths (denoted by λ) that are in the range of $\lambda \gtrsim 2\ell$. One can observe that for directions that do not coincide with the lattice axes, the domains of permissible wavevectors shrink in size and tend towards larger wavelengths (see Figs. 2(a)-(c)). Increasing the angle χ , which amounts to tilting the ciliary beating orbit away from the z -axis, further

accentuates this feature while allowing for the direction of propagation to deviate from the direction of beating, leading to the formation of dexioelectric or laeoelectric metachronism [see Figs. 2(d)-(e)].

To examine the role of the underlying lattice structure, we consider a triangular lattice, which is characterized by reciprocal lattice vectors $\mathbf{G} = \frac{2\pi}{\ell}[(m\mathbf{e}_x + (-m/\sqrt{3} + 2n/\sqrt{3})\mathbf{e}_y)]$, ($m, n \in \mathbb{Z}$). The dispersion relation does not differ appreciably from that of a square lattice, as Fig. 2(f) shows for the case of $\theta = 0$ and $\chi = 0$. However, while for a square lattice the stable wave region is centered around $k_x = \pm\pi/\ell$ and $k_y = 0$, for a triangular lattice it is centered around $k_x = \pm\pi/\ell$ and $k_y = 0$ or $k_x = \pm(2 - \sqrt{3})\pi/\ell$ and $k_y = \pi/\ell$, which means that there will be a phase shift between the neighboring cilia along \mathbf{e}_x direction, hence giving rise to dexioelectric or laeoelectric waves [6]. This behavior can be understood by analyzing the dynamics of two cilia with the appropriate geometric arrangement [45]. We thus find that tuning the orientation of the cilia trajectories and controlling the positioning of the cilia in the array provide the possibility to generate metachronal waves with desired wavelengths and directions of propagation.

We note that in our current formulation the stability criterion is degenerate with respect to the direction of propagation, i.e. $\pm\mathbf{k}$ are both either stable or unstable at the same time. The symmetry can be broken by considering near-field effects in the hydrodynamic interaction between cilia; this will be discussed in future work. Note also that while the stability analysis is performed in terms of $\bar{\phi}$, the one-to-one correspondence in Eq. (8) guarantees that it will also describe the stability of the modes in terms of the original ϕ coordinate.

Agent-based simulation

To support the validity of the above analytical description, which is analyzed within the framework of linear stability analysis, we perform numerical simulations based on the governing dynamical equations of the cilia [Eq. (3)]. The examples of the time evolution are presented in Fig. 3 for an 11×11 cilia array, which is simulated with periodic boundary conditions. The cilia are positioned on a square lattice [Fig. 3(a-e)] with different tilting angles θ and χ , as well as a triangular lattice with $\theta = 0$ and $\chi = 0$ [Fig. 3(f)]. The cilia are all initiated with the same phase $\phi = 0$ at the start of the simulation at $t = 0$. The time interval for each simulation step is $dt/t_0 = 2 \cdot 10^{-3}$, with $t_0 = \eta\ell^2/f_0$ defining a characteristic time.

As can be seen in Fig. 3 and the Supplemental Movies [45], in all cases the cilia coordinate with each other and form a metachronal wave after a transient period. For example, in the case of the cilia on a square lattice with the tilting angles of the trajectory as $\theta = 0$ and $\chi = 0$ [as shown in Fig. 3(a)], the cilia beat in the form of the metachronal wave with the wave vector $k_x \simeq \pi/\ell$ and

$k_y \simeq 0$. In another case, corresponding to $\theta = \pi/4$ and $\chi = 0$, the cilia beat in the form of the metachronal wave with the wavevector $k_x \simeq \pi/2\ell$ and $k_y \simeq \pi/2\ell$. These simulation results agree very well with the prediction of the linear stability analysis; the values of the measured stable waves lie for all cases within the range predicted by the theoretical calculations as presented in Fig. 2.

DISCUSSION

We have constructed a theoretical framework to study metachronal waves in ciliary arrays, where each cilium is driven independently with the same beat pattern and interacts with the others via hydrodynamic interactions for arbitrary geometric configurations. We calculate the dispersion relation of the system, relating the propagation frequency and the wavevector of the metachronal wave, and observe that the frequency is relatively insensitive to the changes in the wavevector. We have found that stable waves correspond to finite domains of wavevector, which are selected with relatively well-defined orientation of propagation that is determined by the geometric characteristics of the ciliary beating pattern and the lattice structure. Our results allow us to predict the role of the different harmonics in the moment decomposition of the beat pattern and the friction, which in turn can be used to make predictions about control of metachronal waves using external cues, as has been demonstrated in the case of phototaxis of *Chlamydomonas* [46].

SYNCHRONIZATION OF TWO CILIA

Consider two cilia rotating in yz plane, and the centre of one cilium trajectory is located at $\mathbf{R}_1 = (0, 0, h)$ with phase ϕ_1 , and the other one is located at $\mathbf{R}_2 = (\ell \cos \Theta, \ell \sin \Theta, h)$ with phase ϕ_2 . The dynamic equation of cilium 1 is,

$$\dot{\phi}_1 = \frac{f(\phi_1)}{\zeta(\phi_1)a} + \frac{1}{a} \mathbf{t}_1 \cdot \mathbf{G}(\mathbf{R}_1; \mathbf{R}_2) \cdot \mathbf{t}_2 f(\phi_2), \quad (15)$$

or alternatively,

$$\dot{\phi}_1 = \frac{f(\phi_1)}{\zeta_0 a} + H_{12} \frac{f(\phi_2)}{\zeta_0 a}, \quad (16)$$

with $H_{12} = \mathbf{t}_1 \cdot \mathbf{G}(\mathbf{R}_1; \mathbf{R}_2) \cdot \mathbf{t}_2 \zeta_0$. After the coordinate transformation introduced in the main text, $\phi \rightarrow \bar{\phi}$, the dynamic equation of cilium 1 can be re-written as:

$$\dot{\bar{\phi}}_1 = \Omega_0 \left[1 + \bar{H}_{12}(\bar{\phi}_1, \bar{\phi}_2) \frac{\bar{f}(\bar{\phi}_2)}{\bar{f}(\bar{\phi}_1)} \right], \quad (17)$$

where $\bar{H}_{12}(\bar{\phi}_1, \bar{\phi}_2) = H_{12}(\phi_1, \phi_2)$ and $\bar{f}(\bar{\phi}_{1,2}) = f(\phi_{1,2})$. $f(\phi) = f_0[1 + A_2 \cos 2\phi + B_2 \sin 2\phi]$ is taken. Then we can obtain

$$\begin{aligned} \dot{\bar{\Delta}} &= \Omega_0 \left[\bar{H}_{12}(\bar{\phi}_1, \bar{\phi}_2) \frac{\bar{f}(\bar{\phi}_2)}{\bar{f}(\bar{\phi}_1)} - \bar{H}_{21}(\bar{\phi}_2, \bar{\phi}_1) \frac{\bar{f}(\bar{\phi}_1)}{\bar{f}(\bar{\phi}_2)} \right] \\ &= \Omega_0 \bar{H}_{12}(\bar{\phi}_1, \bar{\phi}_2) \left[\frac{\bar{f}(\bar{\phi}_2)}{\bar{f}(\bar{\phi}_1)} - \frac{\bar{f}(\bar{\phi}_1)}{\bar{f}(\bar{\phi}_2)} \right], \end{aligned} \quad (18)$$

where $\bar{\Delta} = \bar{\phi}_1 - \bar{\phi}_2$.

In the case of $h \geq \ell \gg a$, the Blake tensor for the cilia on a lattice coordinated as \mathbf{r} can be approximated as:

$$G_{\alpha\beta} \simeq \frac{1}{16\pi^2\eta} \int d^2q \frac{1}{|\mathbf{q}|} e^{i\mathbf{q} \cdot (\mathbf{r}' - \mathbf{r})} \left(2\delta_{\alpha\beta} - \frac{q_\alpha q_\beta}{|\mathbf{q}|^2} \right), \quad (\alpha, \beta = x, y), \quad (19)$$

$$G_{\alpha z} \simeq 0, \quad (20)$$

$$G_{z\alpha} \simeq 0, \quad (21)$$

$$G_{zz} \simeq \frac{1}{16\pi^2\eta} \int d^2q \frac{1}{|\mathbf{q}|} e^{i\mathbf{q} \cdot (\mathbf{r}' - \mathbf{r})}. \quad (22)$$

where we ignore the difference between the projected positions \mathbf{R}_p and the lattice locations \mathbf{r} , as well as fast decaying terms such as $\exp(-|\mathbf{q}|h)$. By taking the Green's function in Equation (19), $\bar{H}_{12}(\bar{\phi}_1, \bar{\phi}_2)$ can be approximated as $\bar{H}_{12}(\bar{\phi}_1, \bar{\phi}_2) = G_{yy} \sin \bar{\phi}_1 \sin \bar{\phi}_2 + G_{zz} \cos \bar{\phi}_1 \cos \bar{\phi}_2$. By taking $\bar{\Sigma} = \bar{\phi}_1 + \bar{\phi}_2$ and averaging over the fast variable $\bar{\Sigma}$ in terms of $\langle \dots \rangle = \frac{1}{4\pi} \int_0^{4\pi} \dots$, then the dynamic equation can be written as

$$\dot{\bar{\Delta}} \simeq (G_{yy} - G_{zz}) B_2 \sin \bar{\Delta} = \frac{\sin^2 \Theta}{\ell} B_2 \sin \bar{\Delta}. \quad (23)$$

Here we introduce an effective potential, which is

$$\begin{aligned} \mathcal{U} &= - \int_0^{\bar{\Delta}} d\bar{\Delta}' \frac{\sin^2 \Theta}{\ell} B_2 \sin \bar{\Delta}' \\ &= \frac{\sin^2 \Theta}{\ell} B_2 \cos(\bar{\Delta} - 1) \simeq \frac{\sin^2 \Theta}{\ell} B_2 (\cos \Delta - 1) \end{aligned} \quad (24)$$

where the local minimum locates at $\Delta = \pi$ as the stable phase shift between the cilia. By assuming the cilia beat with a wave vector \mathbf{k} , then the phase difference is $\Delta = \mathbf{k} \cdot \mathbf{r} = k_x \ell \cos \Theta + k_y \ell \sin \Theta$, so the wave vector should follow $k_x \ell \cos \Theta + k_y \ell \sin \Theta = \pi$.

We are grateful to Andrej Vilfan and Masao Doi for fruitful discussions. This work was supported by the Max-Planck-Gesellschaft. F. M. thanks partial supports from Alexander von Humboldt Foundation, Strategic Priority Research Program of Chinese Academy of Sciences (No. XDA17010504) and the National Natural Science Foundation of China (No. 12047503). R. R. B. Acknowledges a doctoral scholarship from the EPSRC and a University of Bristol Vice-Chancellor's Fellowship.

[1] J. Gray, *Ciliary movement* (Cambridge University Press, 1928).

[2] C. Brennen and H. Winet, Fluid mechanics of propulsion

- by cilia and flagella, *Annual Review of Fluid Mechanics* **9**, 339 (1977).
- [3] R. Golestanian, J. M. Yeomans, and N. Uchida, Hydrodynamic synchronization at low Reynolds number, *Soft Matter* **7**, 3074 (2011).
- [4] S. Camalet, F. Jülicher, and J. Prost, Self-organized beating and swimming of internally driven filaments, *Physical Review Letters* **82**, 1590 (1999).
- [5] R. Ma, G. S. Klindt, I. H. Riedel-Kruse, F. Jülicher, and B. M. Friedrich, Active phase and amplitude fluctuations of flagellar beating, *Physical Review Letters* **113**, 048101 (2014).
- [6] E. W. Knight-Jones, Relations between metachronism and the direction of ciliary beat in metazoa, *Journal of Cell Science* **3**, 503 (1954).
- [7] S. Nonaka, H. Shiratori, Y. Saijoh, and H. Hamada, Determination of left-right patterning of the mouse embryo by artificial nodal flow, *Nature* **418**, 96 (2002).
- [8] A. Takamatsu, K. Shinohara, T. Ishikawa, and H. Hamada, Hydrodynamic Phase Locking in Mouse Node Cilia, *Physical Review Letters* **110**, 248107 (2013).
- [9] R. Faubel, C. Westendorf, E. Bodenschatz, and G. Eichele, Cilia-based flow network in the brain ventricles, *Science* **353**, 176 (2016).
- [10] N. Pellicciotta, E. Hamilton, J. Kotar, M. Faucourt, N. Delgehr, N. Spassky, and P. Cicuta, Entrainment of mammalian motile cilia in the brain with hydrodynamic forces, *Proceedings of the National Academy of Sciences* **117**, 8315 (2020).
- [11] M. B. Short, C. A. Solari, S. Ganguly, T. R. Powers, J. O. Kessler, and R. E. Goldstein, Flows driven by flagella of multicellular organisms enhance long-range molecular transport, *Proc. Natl. Acad. Sci. U.S.A.* **103**, 8315 (2006).
- [12] S. L. Tamm, T. M. Sonneborn, and R. V. Dippell, The role of cortical orientation in the control of the direction of ciliary beat in *Paramecium*, *J. Cell Biol.* **64**, 98 (1975).
- [13] D. R. Brumley, M. Polin, T. J. Pedley, and R. E. Goldstein, Metachronal waves in the flagellar beating of *Volvox* and their hydrodynamic origin, *Journal of The Royal Society Interface* **12**, 20141358 (2015).
- [14] N. Uchida and R. Golestanian, Synchronization and Collective Dynamics in a Carpet of Microfluidic Rotors, *Physical Review Letters* **104**, 178103 (2010).
- [15] N. Uchida and R. Golestanian, Synchronization in a carpet of hydrodynamically coupled rotors with random intrinsic frequency, *EPL (Europhysics Letters)* **89**, 50011 (2010).
- [16] N. Osterman and A. Vilfan, Finding the ciliary beating pattern with optimal efficiency, *Proceedings of the National Academy of Sciences* **108**, 15727 (2011).
- [17] J. Elgeti and G. Gompper, Emergence of metachronal waves in cilia arrays, *Proceedings of the National Academy of Sciences* **110**, 4470 (2013).
- [18] B. A. Evans, A. R. Shields, R. L. Carroll, S. Washburn, M. R. Falvo, and R. Superfine, Magnetically Actuated Nanorod Arrays as Biomimetic Cilia, *Nano Letters* **7**, 1428 (2007).
- [19] M. Vilfan, A. Potocnik, B. Kavcic, N. Osterman, I. Poberaj, A. Vilfan, and D. Babic, Self-assembled artificial cilia, *Proceedings of the National Academy of Sciences* **107**, 1844 (2010).
- [20] N. Coq, A. Bricard, F.-D. Delapierre, L. Malaquin, O. du Roure, M. Fermigier, and D. Bartolo, Collective Beating of Artificial Microcilia, *Physical Review Letters* **107**, 014501 (2011).
- [21] T. Sanchez, D. Welch, D. Nicastro, and Z. Dogic, Cilia-Like Beating of Active Microtubule Bundles, *Science* **333**, 456 (2011).
- [22] F. Meng, D. Matsunaga, J. Yeomans, and R. Golestanian, Magnetically-actuated artificial cilium: A simple theoretical model, *Soft matter* **153**, 3864 (2019).
- [23] E. M. Gauger, M. T. Downton, and H. Stark, Fluid transport at low Reynolds number with magnetically actuated artificial cilia, *The European Physical Journal E* **28**, 231 (2009).
- [24] S. N. Khaderi, C. B. Craus, J. Hussong, N. Schorr, J. Belardi, J. Westerweel, O. Prucker, J. Rühle, J. M. J. den Toonder, and P. R. Onck, Magnetically-actuated artificial cilia for microfluidic propulsion, *Lab on a Chip* **11**, 2002 (2011).
- [25] D. Matsunaga, J. K. Hamilton, F. Meng, N. Bukin, E. L. Martin, F. Y. Ogrin, J. M. Yeomans, and R. Golestanian, Controlling collective rotational patterns of magnetic rotors, *Nature Communications* **10**, 4696 (2019).
- [26] R. Dreyfus, J. Baudry, M. L. Roper, M. Fermigier, H. a. Stone, and J. Bibette, Microscopic artificial swimmers, *Nature* **437**, 862 (2005).
- [27] B. Guirao and J.-F. Joanny, Spontaneous Creation of Macroscopic Flow and Metachronal Waves in an Array of Cilia, *Biophysical Journal* **92**, 1900 (2007).
- [28] D. R. Brumley, K. Y. Wan, M. Polin, and R. E. Goldstein, Flagellar synchronization through direct hydrodynamic interactions, *Elife* **3**, e02750 (2014).
- [29] B. Guirao, A. Meunier, S. Mortaud, A. Aguilar, J.-M. Corsi, L. Strehl, Y. Hirota, A. Desoeuvre, C. Boutin, Y.-G. Han, Z. Mirzadeh, H. Cremer, M. Montcouquiol, K. Sawamoto, and N. Spassky, Coupling between hydrodynamic forces and planar cell polarity orients mammalian motile cilia, *Nature Cell Biology* **12**, 341 (2010).
- [30] A. Vilfan and F. Jülicher, Hydrodynamic Flow Patterns and Synchronization of Beating Cilia, *Physical Review Letters* **96**, 058102 (2006).
- [31] B. Qian, H. Jiang, D. A. Gagnon, K. S. Breuer, and T. R. Powers, Minimal model for synchronization induced by hydrodynamic interactions, *Physical Review E* **80**, 061919 (2009).
- [32] N. Uchida and R. Golestanian, Generic Conditions for Hydrodynamic Synchronization, *Physical Review Letters* **106**, 058104 (2011).
- [33] N. Uchida and R. Golestanian, Hydrodynamic synchronization between objects with cyclic rigid trajectories, *The European Physical Journal E* **35**, 135 (2012).
- [34] A. Maestro, N. Bruot, J. Kotar, N. Uchida, R. Golestanian, and P. Cicuta, Control of synchronization in models of hydrodynamically coupled motile cilia, *Communications Physics* **1**, 28 (2018).
- [35] N. Naremsatsu, R. Quek, K.-H. Chiam, and Y. Iwamoto, Ciliary metachronal wave propagation on the compliant surface of paramecium cells, *Cytoskeleton* **72**, 633 (2015).
- [36] K. Y. Wan and R. E. Goldstein, Coordinated beating of algal flagella is mediated by basal coupling, *Proceedings of the National Academy of Sciences* **113**, E2784 (2016).
- [37] Y. Liu, R. Claydon, M. Polin, and D. R. Brumley, Transitions in synchronization states of model cilia through basal-connection coupling, *Journal of The Royal Society Interface* **15**, 20180450 (2018).
- [38] S. Gueron, K. Levit-Gurevich, N. Liron, and J. J. Blum,

- Cilia internal mechanism and metachronal coordination as the result of hydrodynamical coupling, *Proceedings of the National Academy of Sciences* **94**, 6001 (1997).
- [39] Y. W. Kim and R. R. Netz, Pumping Fluids with Periodically Beating Grafted Elastic Filaments, *Physical Review Letters* **96**, 158101 (2006).
- [40] Y. Ding, J. C. Nawroth, M. J. McFall-Ngai, and E. Kanso, Mixing and transport by ciliary carpets: a numerical study, *Journal of Fluid Mechanics* **743**, 124 (2014).
- [41] C. Wollin and H. Stark, Metachronal waves in a chain of rowers with hydrodynamic interactions, *The European Physical Journal E* **34**, 42 (2011).
- [42] A. Ghorbani and A. Najafi, Symplectic and antiplectic waves in an array of beating cilia attached to a closed body, *Physical Review E* **95**, 052412 (2017).
- [43] D. R. Brumley, M. Polin, T. J. Pedley, and R. E. Goldstein, Hydrodynamic Synchronization and Metachronal Waves on the Surface of the Colonial Alga *Volvox carteri*, *Physical Review Letters* **109**, 268102 (2012).
- [44] J. R. Blake, A note on the image system for a stokeslet in a no-slip boundary, *Mathematical Proceedings of the Cambridge Philosophical Society* **70**, 303 (1971).
- [45] See Supplemental Material at [URL] for some details of the calculation, the and a video that shows how a metachronal wave emerges in our simulation.
- [46] R. R. Bennett and R. Golestanian, A steering mechanism for phototaxis in *chlamydomonas*, *Journal of The Royal Society Interface* **12**, 20141164 (2015).

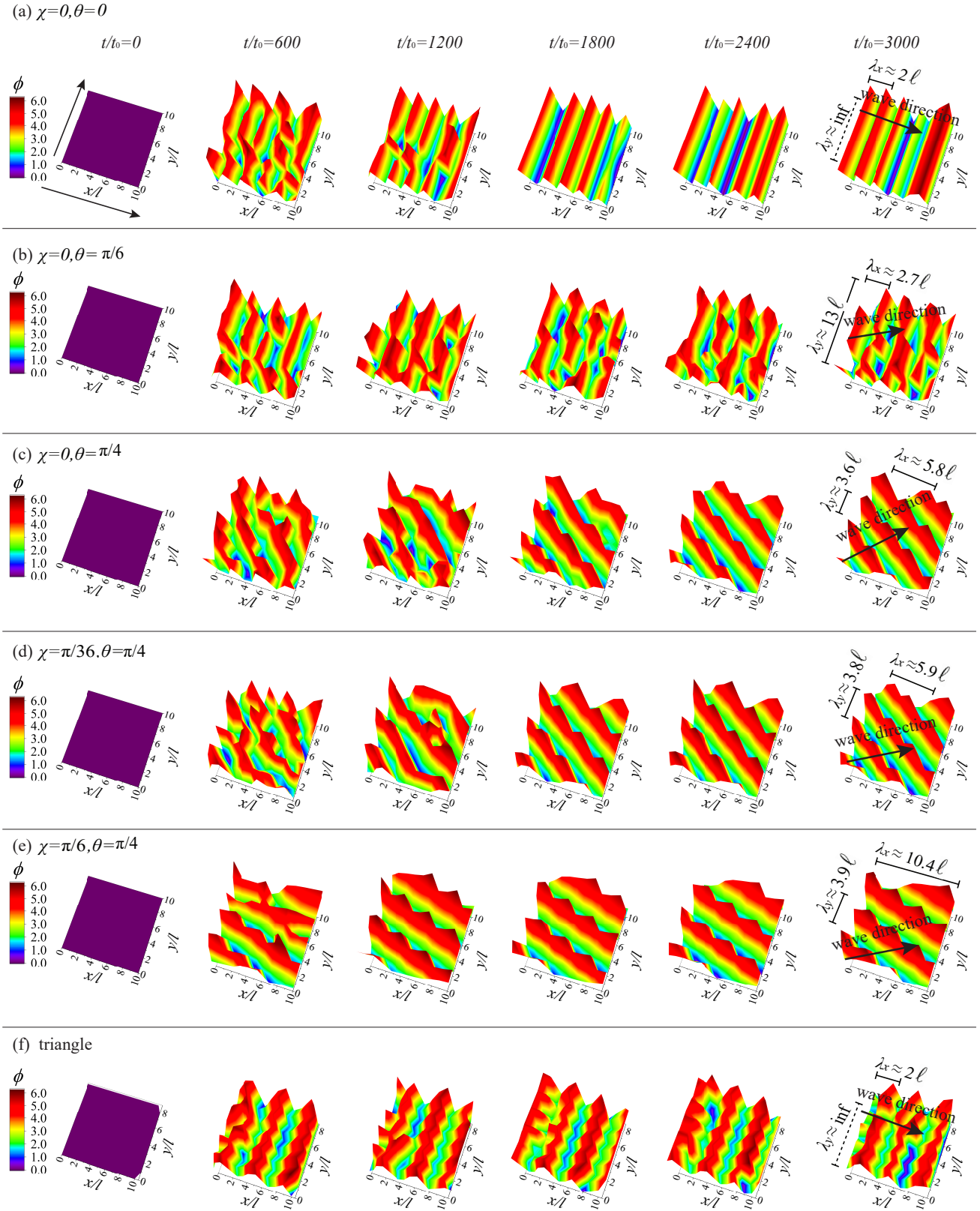


FIG. 3. Simulation snapshots showing how the phases that represent the cilia beating cycle evolve with time in an 11×11 array, where the cilia rotate along the trajectory defined by the angles: (a) $\chi = 0, \theta = 0$, (b) $\chi = 0, \theta = \pi/6$, (c) $\chi = 0, \theta = \pi/4$, (d) $\chi = \pi/36, \theta = \pi/4$ and (e) $\chi = \pi/6, \theta = \pi/4$ (see Fig. 1). Panel (f) corresponds to a triangular lattice with $\chi = 0, \theta = 0$. Other parameters for panels (a)-(f) are: $a = 0.2\ell, b = 0.05\ell, h = \ell, A_2 = 0.5, B_2 = 0.5, C_2 = 0$, and $D_2 = 0$. The characteristic time scale is $t_0 = \eta\ell^2/f_0$. The measured wavelengths and direction of propagation are shown on the last column; in every case the resulting wavevector lies within the range of the stable wave modes from the corresponding panels of Fig. 2.